

PAPER • OPEN ACCESS

## Transverse extension of partons in the proton probed by DVCS at COMPASS

To cite this article: Andrzej Sandacz and the COMPASS Collaboration 2020 *J. Phys.: Conf. Ser.* **1435** 012046

View the [article online](#) for updates and enhancements.



**IOP | ebooks™**

Bringing you innovative digital publishing with leading voices to create your essential collection of books in STEM research.

Start exploring the collection - download the first chapter of every title for free.

# Transverse extension of partons in the proton probed by DVCS at COMPASS

Andrzej Sandacz<sup>1</sup>  
(on behalf of the COMPASS Collaboration)

Division of High Energy Physics, National Centre for Nuclear Research, PL 02-093 Warsaw, Poland

E-mail: Andrzej.Sandacz@ncbj.gov.pl

**Abstract.** We present the first result on exclusive single-photon muoproduction on the proton in the range of intermediate values of the Bjorken variable  $x_{Bj}$ , which was recently published by COMPASS collaboration. The measurements were performed using 160 GeV/c polarised  $\mu^+$  and  $\mu^-$  beams of the CERN SPS scattering off a liquid hydrogen target. We determine the dependence of the average of the measured  $\mu^+$  and  $\mu^-$  cross sections for deeply virtual Compton scattering on the squared four-momentum transfer  $t$  from the initial to the final proton. The slope  $B$  of the  $t$ -dependence is fitted with a single exponential function, which yields  $B = (4.3 \pm 0.6_{\text{stat}} \pm 0.1_{\text{sys}}) (\text{GeV}/c)^{-2}$ . This result can be converted into an average transverse extension of partons in the proton,  $\sqrt{\langle r_{\perp}^2 \rangle} = (0.58 \pm 0.04_{\text{stat}} \pm 0.01_{\text{sys}}) \text{fm}$ . For this measurement, the average virtuality of the photon mediating the interaction is  $\langle Q^2 \rangle = 1.8 (\text{GeV}/c)^2$  and the average value of the Bjorken variable is  $\langle x_{Bj} \rangle = 0.056$ . We also compare COMPASS result to earlier estimates at very small  $x_{Bj}$  from HERA.

## 1. Introduction

The high energy polarised muon beam available at CERN, with positive or negative charge, makes COMPASS a unique place for studies of General Parton Distributions (GPDs). The theoretical framework of General Parton Distributions (GPDs) [1, 2, 3] provides a novel description of the nucleon's partonic structure. In particular, GPDs allow a description of the nucleon as an extended object, sometimes referred to as a 3-dimensional 'nucleon tomography' [4], which correlates (transverse) spatial and (longitudinal) momentum degrees of freedom. From the theoretical perspective the most straightforward way to study the 'nucleon tomography' is the process of Deeply Virtual Compton Scattering (DVCS). A comprehensive experimental overview of DVCS is presented in Ref. [5] and results of a recent phenomenological studies and predictions for DVCS can be found in Ref. [6].

In this contribution, we present the COMPASS result from Ref. [7] on the measurement of the DVCS cross section obtained by studying exclusive single-photon production in muon-proton scattering,  $\mu p \rightarrow \mu' p' \gamma$ . Following Refs. [4, 8, 9, 10], the slope  $B$  of the measured exponential  $t$ -dependence of the differential DVCS cross section can be approximately converted into the

<sup>1</sup> Work supported by the Polish NCN Grant 2017/26/M/ST2/00498.



average squared transverse extension of partons in the proton as probed by DVCS,

$$\langle r_{\perp}^2(x_{Bj}) \rangle \approx 2\langle B(x_{Bj}) \rangle \hbar^2, \quad (1)$$

which is measured at the average value of  $x_{Bj}$  accessed by COMPASS. Here,  $t$  is the squared four-momentum transferred to the target proton and  $x_{Bj}$  is the Bjorken variable. The quantity  $r_{\perp}$  is the transverse distance between the active quark and the centre of momentum of the spectator quarks and is hence used in this article to represent the transverse extension of partons in the proton.

## 2. Experimental set-up

COMPASS is a fixed-target experiment situated at the M2 beam-line of the CERN SPS. It can deliver either hadron or naturally polarised muon beams of a given charge in the energy range between 50 and 280 GeV. For the GPD program the data are collected with the muon beam nominal energy of 160 GeV and with muons of both polarities:  $\mu^+$  ( $\mu^-$ ) with polarisation of about -0.8 (+0.8).

The COMPASS apparatus [11, 12] consists of a two-stage forward spectrometer comprising various tracking detectors, electromagnetic and hadronic calorimeters, muon identification detectors, and a ring imaging Cherenkov counter grouped around two dipole magnets SM1 and SM2. For the GPD program the set-up was complemented by installing a large proton recoil detector CAMERA around the 2.5 m long liquid hydrogen target and a large-angle electromagnetic calorimeter ECAL0. The 4-meter long CAMERA consists of two concentric barrels, each of 24 scintillator slats with a read out at both ends. The recoil proton detection is based on the ToF measurement between the two barrels. The calorimeter ECAL0 that is situated just downstream of CAMERA allows to extend the accessible kinematic domain for DVCS and exclusive  $\pi^0$  production towards higher  $x_{Bj}$ , improve hermeticity for detection of exclusive events and reduce the background to single-photon events production, which originates from  $\pi^0$  and other decays.

## 3. Data analysis

The data used for this analysis were recorded by COMPASS experiment during four weeks pilot run in 2012. The selected events are required to have at least one reconstructed vertex inside the liquid-hydrogen target associated with an incoming muon and a single outgoing muon of the same charge, a recoil proton candidate and exactly one "neutral cluster" detected above 4 GeV, 5 GeV or 10 GeV thresholds in electromagnetic calorimeters ECAL0, ECAL1 or ECAL2, respectively. Here, neutral cluster specifies a cluster not associated to a charged particle. For ECAL0 any cluster is considered as neutral, as there are no tracking detectors in front. The spectrometer information on incoming and scattered muons, as well as on position and energy measured for the neutral cluster, is used together with measured information from the time-of-flight system of the target-recoil detector. For a given event, the variables for recoil proton candidates are compared with the corresponding predictions that are obtained using spectrometer information only.

Exemplary results of this comparison are displayed in Fig. 1 using two variables that characterize the kinematics of the recoiling target particle. Figure 1(a) shows the difference between the measured and the predicted azimuthal angle,  $\Delta\Phi$ , and Fig. 1(b) the difference between the measured and the predicted transverse momentum,  $\Delta p_T$ .

Figure 1 shows additionally a comparison between the data and the sum of Monte Carlo yields that includes all single-photon production mechanisms, i.e. BH, DVCS and their interference,

as well as the  $\pi^0$  background estimates. The background originating from  $\pi^0$  production, where one photon of the  $\pi^0$  decay remains undetected, is estimated using a Monte Carlo simulation. This simulation, which is denoted as  $\pi^0$  background in Fig.1, is the sum of two components. First, the HEPGEN generator [13, 14] is used with the parameterisation of Ref. [15] for the cross section of the exclusive reaction  $\mu p \rightarrow \mu p \pi^0$ . Secondly, the LEPTO 6.5.1 generator with the COMPASS tuning is used to simulate the tail of non-exclusive  $\pi^0$  production, which is accepted by our experimental selections.

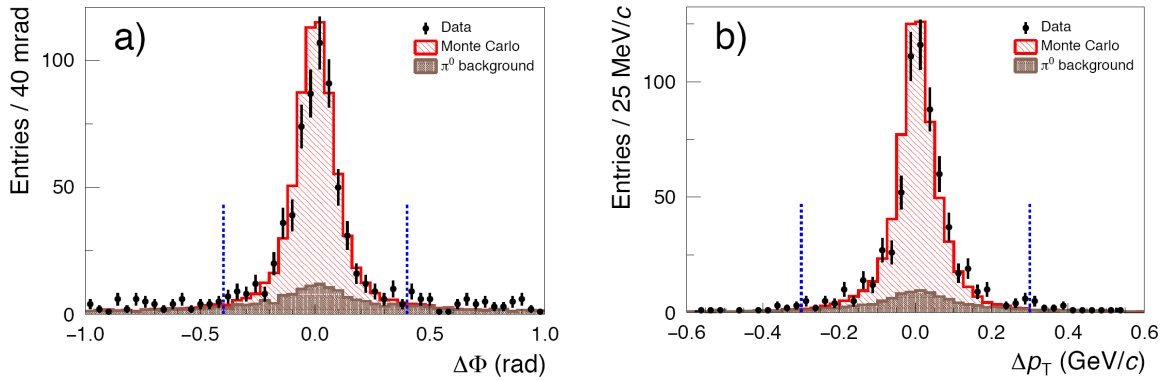


Figure 1: Distribution of the difference between predicted and reconstructed values of (a) the azimuthal angle and (b) the transverse momentum of the recoiling proton candidates for  $1 (\text{GeV}/c)^2 < Q^2 < 5 (\text{GeV}/c)^2$ ,  $0.08 (\text{GeV}/c)^2 < |t| < 0.64 (\text{GeV}/c)^2$  and  $10 \text{ GeV} < \nu < 32 \text{ GeV}$ . The dashed blue vertical lines enclose the region accepted for analysis. Here, Monte Carlo also includes  $\pi^0$  background. Figure from Ref. [7].

After the application of the selection criteria a kinematic fit is performed, which is constrained by requiring a single-photon final state in order to obtain the best possible determination of all kinematic parameters in a given event.

In this analysis we determine the differential cross section for muon-induced single-photon production

$$d\sigma := \frac{d^4\sigma^{\mu p \rightarrow \mu' p' \gamma}}{dQ^2 d\nu dt |d\phi} \quad (2)$$

measured separately using either a  $\mu^+$  or a  $\mu^-$  beam of  $160 \text{ GeV}/c$  average momentum. Here,  $Q^2$  and  $\nu$  denote the virtual photon virtuality and its energy in the lab. system,  $t$  is the square of the four-momentum transfer between the target and recoil protons and  $\phi$  is the azimuthal angle between the lepton scattering plane and the photon production plane. Details on the extraction of the cross sections, applied experimental corrections and discussion of systematic uncertainties can be found in Refs. [7, 16].

Denoting charge and helicity of an incident  $\mu^+$  ( $\mu^-$ ) beam by  $+$  ( $-$ ) and  $\leftarrow$  ( $\rightarrow$ ), respectively, the sum of the cross sections for  $\mu^+$  and  $\mu^-$  beams reads:

$$2 d\sigma \equiv d\sigma^{\leftarrow+} + d\sigma^{\rightarrow-} = 2(d\sigma^{BH} + d\sigma^{DVCS} - |P_\mu| d\sigma^I). \quad (3)$$

Here,  $P_\mu$  denotes the polarisation of the muon beam. The single-photon final state in lepton-nucleon scattering can also originate from the Bethe-Heitler (BH) process, i.e. photon emission from either the incoming or the outgoing lepton. Hence the DVCS and BH processes interfere, so that the above sum of  $\mu^+$  and  $\mu^-$  cross sections comprises not only the contributions  $d\sigma^{DVCS}$  and  $d\sigma^{BH}$  but also that from the interference term denoted by  $d\sigma^I$ .

After subtracting the cross section of the BH process,  $d\sigma^{BH}$ , from Eq. (3) and integrating the remainder over  $\phi$ , all azimuth-dependent terms disappear and only the dominant contribution from transversely polarised virtual photons to the DVCS cross section remains. It is indicated by the subscript T:

$$\frac{d^3\sigma_T^{\mu p}}{dQ^2 d\nu dt} = \int_{-\pi}^{\pi} d\phi (d\sigma - d\sigma^{BH}). \quad (4)$$

This cross section is converted into the cross section for virtual-photon scattering using the flux  $\Gamma(Q^2, \nu, E_\mu)$  for transverse virtual photons [7, 16]:

$$\frac{d\sigma^{\gamma^* p}}{dt} = \frac{1}{\Gamma(Q^2, \nu, E_\mu)} \frac{d^3\sigma_T^{\mu p}}{dQ^2 d\nu dt}. \quad (5)$$

#### 4. Results and discussion

The  $t$ -dependence of the extracted cross section is shown in Fig. 2. The presented cross section is averaged over the kinematic range  $1 (\text{GeV}/c)^2 < Q^2 < 5 (\text{GeV}/c)^2$  and  $10 \text{ GeV} < \nu < 32 \text{ GeV}$ . The observed  $t$ -dependence of the DVCS cross section can be described by a single-exponential function  $e^{-B|t|}$ . The four data points are fitted using a binned maximum-likelihood method, where the weights take into account all experimental corrections. The result on the  $t$ -slope,

$$B = (4.3 \pm 0.6_{\text{stat}} \pm 0.1_{\text{sys}}) (\text{GeV}/c)^{-2}, \quad (6)$$

is obtained at the average kinematics  $\langle W \rangle = 5.8 \text{ GeV}/c^2$ ,  $\langle Q^2 \rangle = 1.8 (\text{GeV}/c)^2$  and  $\langle x_{Bj} \rangle = 0.056$ .

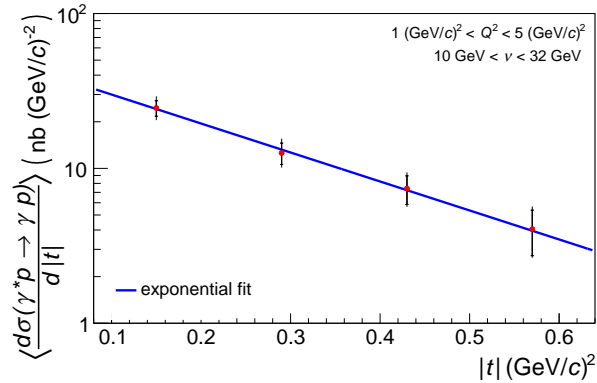


Figure 2: Differential DVCS cross section as a function of  $|t|$ . The mean value of the cross section is shown at the centre of each of the four  $|t|$ -bins. The blue curve is the result of a binned maximum likelihood fit of an exponential function to the data. This fit integrates the exponential model over the respective  $t$ -bins and does not use their central values, which are used for illustration only. The probability to observe a similar or better agreement of the data with the blue curve is approximately 7%. Here and in the next figure, inner error bars represent statistical uncertainties and outer error bars the quadratic sum of statistical and systematic uncertainties. Figure from Ref. [7].

Using Eq. (1), the fitted slope  $B$  of the measured  $t$ -dependence of the DVCS cross section is converted into the transverse extension of partons in the proton, as probed by DVCS at about  $\langle x_{Bj} \rangle / 2 = 0.028$ :

$$\sqrt{\langle r_{\perp}^2 \rangle} = (0.58 \pm 0.04_{\text{stat}} \pm 0.01_{\text{sys}} \pm 0.04_{\text{model}}) \text{ fm}. \quad (7)$$

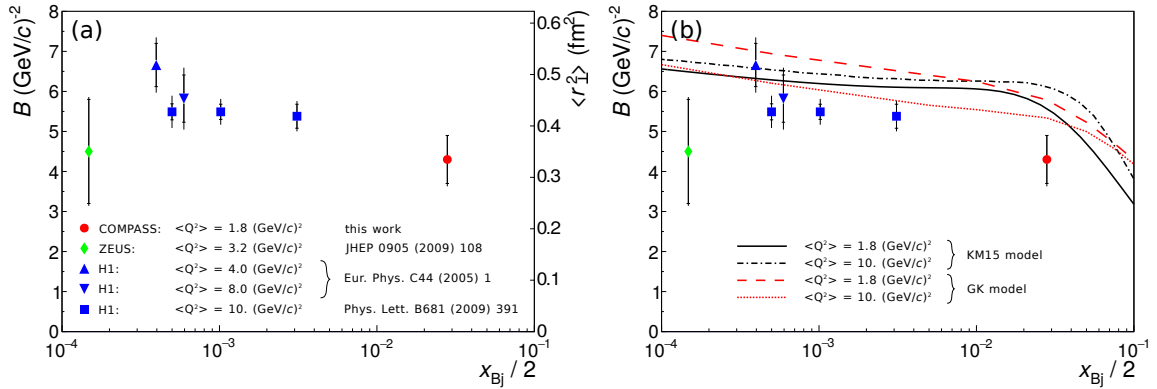


Figure 3: (a) Results from COMPASS and previous measurements by H1 [18] and ZEUS [19] on the  $t$ -slope parameter  $B$ , or equivalently the average squared transverse extension of partons in the proton,  $\langle r_{\perp}^2 \rangle$ , as probed by DVCS at the proton longitudinal momentum fraction  $x_{Bj}/2$  (see text). Inner error bars represent statistical and outer ones the quadratic sum of statistical and systematic uncertainties. (b) Same results compared to the predictions of the GK [20, 21, 17] and KM15 [22, 23] models. Figure is the corrected Fig. 5 from Ref. [7].

The determination of the model uncertainty is explained below. Figure 3 (a) shows our result together with those obtained by earlier high-energy experiments that used the same method to determine the DVCS cross section and extract the  $t$ -slope parameter  $B$ , or equivalently the average squared transverse extension of partons in the proton,  $\langle r_{\perp}^2 \rangle$ . We note that the results of the HERA collider experiments H1 [18] and ZEUS [19] were obtained at higher values of  $Q^2$  as compared to that of the COMPASS measurement. Also, while our measurement probes the transverse extension of partons in the proton in the intermediate  $x_{Bj}$  range, the measurements at HERA are sensitive to values of  $x_{Bj}/2$  below  $10^{-2}$ .

As described e.g. in Ref. [10], the slope  $B$  of the  $t$ -dependence of the DVCS cross section can be converted into the transverse extension of partons in the proton assuming: i) the dominance of the imaginary part of the Compton Form Factor (CFF)  $\mathcal{H}$ , and ii) a negligible effect of a non-zero value of the skewness  $\xi$ , which is defined as one half of the longitudinal momentum fraction transferred between the initial and final proton and is approximately equal to  $x_{Bj}/2$  at small values of  $x_{Bj}$ .

In the following, we interpret our measurement of the  $B$ -slope at leading order in  $\alpha_S$  and at leading twist. In such a case, the spin-independent DVCS cross section is only sensitive to the quantity  $c_0^{DVCS}$  that is related at small  $x_{Bj}$  to the CFFs  $\mathcal{H}$ ,  $\tilde{\mathcal{H}}$  and  $\mathcal{E}$  as [24]:

$$c_0^{DVCS} \propto 4(\mathcal{H}\mathcal{H}^* + \tilde{\mathcal{H}}\tilde{\mathcal{H}}^*) + \frac{t}{M^2}\mathcal{E}\mathcal{E}^*. \quad (8)$$

In the  $x_{Bj}$ -domain of COMPASS,  $c_0^{DVCS}$  is dominated by the imaginary part of the CFF  $\mathcal{H}$ .

In this region, the contributions by the real part of  $\mathcal{H}$  and by other CFFs amount to about 3% when calculated using the GK model [20, 21, 17] ported to the PARTONS framework [25] and to about 6% when using the KM15 model [22, 23]. Using the second value, the systematic model uncertainty related to assumption i) above is estimated to be about  $\pm 0.03$  fm.

A strict relation between the slope  $B$  and  $\langle r_{\perp}^2 \rangle$  only exists for  $\xi = 0$ . A non-zero value of  $\xi$  introduces an additional uncertainty on  $\langle r_{\perp}^2 \rangle$  that is related to a shift of the centre of the reference system, in which  $\langle r_{\perp}^2 \rangle$  is defined [26]. Using the GK model, we estimate the corresponding systematic uncertainty regarding assumption ii) above to be about  $\pm 0.02$  fm. The value for the model uncertainty given in Eq. 7 is obtained by quadratic summation of the two components.

The same data as presented in Fig. 3 (a) are shown in Fig. 3 (b), compared to calculations of the phenomenological GK and KM15 models for the data in the low and medium  $x_{Bj}$  range.

Even taking into account the relatively small effect of  $Q^2$  evolution, some scale offset between data and models seems to exist. When comparing our result on the transverse extension of partons in the proton to the lowest- $Q^2$  result of H1, there is an indication for shrinkage, i.e. a decrease of the B-slope with  $x_{Bj}$ , at the level of about 2.5 standard deviations of the combined uncertainty.

In order to reliably determine the full  $x_{Bj}$ -dependence of the transverse extension of partons in the proton, global phenomenological analyses using results from DVCS experiments at HERA, CERN, and JLab have been performed to pin down the imaginary part of CFF  $\mathcal{H}$ , and eventually the GPD  $H$  itself.

## 5. Outlook

In 2016 and 2017 the COMPASS collaboration has collected a large data sample on the GPD program. An expected increase of the statistic is by a factor of about 10 compared to the 2012 data. An investigation of GPDs with DVCS using the data from 2016-2017 will allow us to determine the  $x_{Bj}$ -dependence of  $t$ -slope of the differential cross sections. The measurements of the azimuthal angle dependence for the beam charge and spin sum and difference of single- $\gamma$  cross sections will give access to the real and imaginary parts of the DVCS amplitude, and will allow to further constrain GPDs  $H$ . Studies of exclusive production of vector mesons ( $\rho^0$ ,  $\omega$ ,  $\phi$ ) will lead to the quark flavour and gluon separation for GPDs  $H$ , while that of exclusive  $\pi^0$  production will provide constraints on chiral-odd GPDs.

## References

- [1] Müller D *et al* 1994 *Fortsch. Phys.* **42** 101
- [2] Ji X 1997 *Phys. Rev. Lett.* **78** 610; 1997 *Phys. Rev. D* **55** 7114
- [3] Radyushkin A V 1996 *Phys. Lett. B* **385** 333; 1997 *Phys. Rev. D* **56** 5524
- [4] Burkardt M 2000 *Phys. Rev. D* **62** 071503; 2002 erratum-ibid. *D* **66** 119903; 2003 *Int. J. Mod. Phys. A* **18** 173; 2004 *Phys. Lett. B* **595** 245
- [5] d'Hose N, Nicolai S and Rostomyan A 2016 *Eur. Phys. J. A* **52** 151
- [6] Kumerički K, Liuti S. and Moutarde H 2016 *Eur. Phys. J. A* **52** 157
- [7] Akhunzyanov R *et al.* (COMPASS Collaboration) 2019 *Phys. Lett. B* **793** 188
- [8] Frankfurt L, Strikman M and Weiss C 2005 *Ann. Rev. Nucl. Part. Sci.* **55** 403
- [9] Aschenauer E C, Fazio S, Kumerički K and Müller D 2013 *JHEP* **09** 93
- [10] Moutarde H, Sznajder P and Wagner J 2018 *Eur. Phys. J. C* **78** 890
- [11] Abbon P *et al.* (COMPASS Collaboration) 2007 *Nucl. Instr. Meth. A* **577** 455
- [12] Abbon P *et al.* (COMPASS Collaboration) 2015 *Nucl. Instr. Meth. A* **779** 69
- [13] Sandacz A and Sznajder P 2012 *HEPGEN - generator for hard exclusive leptonproduction* arXiv:1207.0333 [hep-ph]
- [14] Regali C 2016 PhD thesis, University of Freiburg, DOI: 10.6094/UNIFR/11449; Szameitat T 2017 PhD thesis, University of Freiburg, DOI: 10.6094/UNIFR/11686
- [15] Goloskokov S V and Kroll P 2011 *Eur. Phys. J. A* **47** 112
- [16] Jörg P 2017 PhD thesis, University of Freiburg, DOI: 10.6094/UNIFR/12397; 2018 *Exploring the Size of the Proton* Springer International Publishing, DOI: 10.1007/978-3-319-90290-6
- [17] Goloskokov S V and Kroll P 2010 *Eur. Phys. J. C* **65** 137
- [18] Aaron F D *et al.* (H1 Collaboration) 2009 *Phys. Lett. B* **681** 391; Aktas A *et al.* (H1 Collaboration) 2005 *Eur. Phys. J. C* **44** 1
- [19] Chekanov S *et al.* (ZEUS Collaboration) 2009 *JHEP* **0905** 108
- [20] Goloskokov S V and Kroll P 2005 *Eur. Phys. J. C* **42** 281
- [21] Goloskokov S V and Kroll P 2008 *Eur. Phys. J. C* **53** 367
- [22] Kumerički and Müller D 2010 *Nucl. Phys. B* **841** 1
- [23] Kumerički and Müller D 2016 *EPJ Web Conf.* **112** 01012
- [24] Belitsky A V, Müller D and Kirchner A 2002 *Nucl. Phys. B* **629** 323
- [25] Berthou B *et al.* 2018 *Eur. Phys. J. C* **78** 478
- [26] Diehl M 2002 *Eur. Phys. J. C* **25** 223; 2003 *Eur. Phys. J. C* **31** 277(i)